Nuclear Engineering and Technology 51 (2019) 1169–1175

Contents lists available at ScienceDirect

Nuclear Engineering and Technology

journal homepage: www.elsevier.com/locate/net

Technical Note

Minimum detectable activity of plastic scintillator for in-situ beta measurement system in ground water

Woo Nyun Choi, UkJae Lee, Jun Woo Bae, Hee Reyoung Kim*

Nuclear Engineering, Ulsan National Institute of Science and Technology, 50, UNIST-gil, Ulsan, 44919, Republic of Korea

ARTICLE INFO

Article history:
Received 6 November 2018
Received in revised form
11 January 2019
Accepted 1 February 2019
Available online 1 February 2019

Keywords:
Groundwater monitoring
Gross beta measurements
Tritium
On-site measurement
Minimum detectable activity

ABSTRACT

The minimum detectable activity (MDA) value was derived according to the flow rate of the sample and degree of amplification of the device by sending the sample directly from the collection site to the detection part through a pump. This method can lead to reduction in time and cost compared to the existing measurement method that uses a pre-treatment process. In this study, experiments were conducted on ^{3}H and ^{90}Sr, which are the major pure beta-emitting radionuclides, by setting the sample flow rate and the amplification gain as factors. The MDA values were derived according to the flow rates, considering that the flow rate can affect the MDA values. There were no change in the MDA under different flow rates of 0, 600, 800, and 1000 mL/min. Therefore, it was confirmed that the flow rate may not be considered when collecting samples for monitoring in actual field. As the degree of amplification of the amplifier increased, the time required to reach the target MDA decreased. When the amplification was quadrupled, the detection efficiency increased by approximately 23.4 times, and the time to reach the MDA decreased to approximately 1/550 times. This method offers the advantage of real-time on-site monitoring.

1. Introduction

Periodic monitoring of site ground water before and after decontamination and decommissioning (D & D) of nuclear facilities is necessary; in the case of restricted release after restoration of D & D sites, long-term groundwater radiation monitoring is required. Beta radionuclides generated from nuclear facilities must be managed from the viewpoint of health physics, and technology that can quickly and accurately detect the degree of contamination is required. However, as low-energy beta radionuclide has a short range, it is necessary to use a measuring instrument such as liquid scintillation counter (LSC) during pre-treatment after sampling; LSCs cannot be used in situ when long sampling and analysis times, including pre-treatment, are required [1].

In Korea, gross beta measurements have not been considered in relation to water until recently. Therefore, the in-situ beta measurement system was attempted to develop for beta measurements at D&D sites. Plastic scintillators have demonstrated high sensitivity in detecting short-range beta radiation with minimal damage during contact with water; on the basis of this concept a system for monitoring short-range beta radiation in groundwater in D&D sites was proposed [2].

It takes a long time to detect radiation using devices such as LSCs. However, plastic scintillators for in situ beta measurement system in ground water have advantages in terms of reduction in time and cost. In this method, the flow rate can vary, as the sample is supplied to the detector part through a pump. In the MDA equation, the MDA is affected by the background count rate, detection time, detection efficiency which is consisted of gross count rate, background count rate and activity, and sample volume [2,3]. It was considered that the concentration of radioactive contamination of the sample may not be uniformly distributed and the variation in the flow rates can cause the gross count rate to be different at each measurement point, which can affect the detection efficiency and consequently the MDA. Therefore, it is necessary to investigate these characteristics in this study and the flow rate is set as a variable. In addition, the amplification characteristics of the amplifiers were derived and an in-situ beta measurement system for groundwater was designed. In general, an increase in the degree of amplification can change both the background and gross count rates, which affects detection efficiency.

* Corresponding author.
E-mail address: kimhr@unist.ac.kr (H.R. Kim).

https://doi.org/10.1016/j.net.2019.02.001

2. Methods

2.1. Concept of in situ beta monitoring with scintillator

A detection system that directly connects the radiation source with the plastic scintillator was designed for detection of short-range beta radiations [4]. The plastic scintillator used in this experiment is physically and chemically stable, has minimal damage even when directly exposed to water, and has relatively low back scattering due to its low effective atomic number. The detection time can be reduced on the basis of the design of the detection part owing to the increased detection efficiency. Fig. 1 shows a schematic of the in-situ beta monitoring system.

2.2. Manufacture of acrylic scintillator support structure

The distance between the scintillator and radiation source was determined as the main efficiency parameter, and the water-sample height, scintillator diameter and thickness, and air-layer thickness between the scintillator and water sample were determined by MCNP 6 simulation. These measurements were used to optimize the design of the scintillator. As the height of the water sample increased, the efficiency decreased; however, the diameter of the scintillator did not have a significant influence on the efficiency, as observed in Fig. 2. In addition, the efficiency decreased as the air-layer thickness increased. The thickness of the scintillator did not significantly influence the efficiency.

The acrylic scintillator support structure was designed and manufactured with dimensions of 60 × 60 × 50 mm^3 (width × length × height) to optimize photon collection in ground water. The height of the water sample was approximately 2 cm, considering the diameter of the silicon tube. The diameter of the scintillator was as close as possible to that of the photo multiplier tube (PMT) area, which is 51 mm in diameter. The scintillator and sample were directly connected such that the air layer was not present. The thickness of the scintillator was set as 1 mm.

2.3. Experimental setup

The high amplification applied to the 855 dual amplifier and noise generated from the PMT owing to the amount of light significantly influence the background count rate. Therefore, the electronics were designed according to the time-delay coincidence circuit to eliminate background noise. In the coincidence circuit, the signals are recognized simultaneously in each PMT. Therefore, both PMTs can recognize the wrong signal due to unexpected background. However, if a delay is applied to the input time of one PMT, the time-delay coincidence circuit can remove such background because an unexpected background will not be recognized in the other PMT. Details of each component are shown in Fig. 3 [5]. The 556 high-voltage power supply applies power to the 276 p.m. base/preamplifier; then, the 855 dual amplifier performs photon amplification. The 551 timing single channel analyzer (SCA) sets the delay time, and the photons are converted to signal form after passing through the 567 time-to-amplitude converter (TAC). The 556 high-voltage power supply can range from 0 kV to 3 kV in kV units and from 0 mA to 10 mA in mA units. It is necessary to supply the appropriate amount of power to the preamplifier and PMT. In this experiment, a power of 1.25 kV was set [6]. The PMT R878 model by Hamamatsu Photonics was used for the experiment [7]. The amplification of the 855 dual amplifier was determined by the coarse and fine gains [8]. The 551 timing SCA sets the delay time, which is the most important parameter in the time-delay coincidence circuit. The total spectrum area was set to 500 ns using the 567 TAC, and the delay time between two PMT signals was set to 250 ns; therefore, the signals were collected near 512 channels corresponding to a delay time of 250 ns to collect the incoming signals simultaneously [9]. Finally, the spectra were analyzed using an EASY-Multichannel Analyzer 2k [10]. An example of the spectrum is shown in Fig. 4.

It is also important to minimize the influence of light during the actual experiment and remove noise signals generated from the PMT as much as possible using the time-delay coincidence circuit. To achieve this, a dark box with dimensions of 800 × 500 × 250 mm^3 (width × length × height) was used, which contains two PMTs. Two RS-232 adapters (DSUB 9 standard), two SHV adapters (φ13 mm), and two BNC adapters (φ12.7 mm) were installed on both sides of the dark box to block light from outside. RS-232 is a power-supply cable connected to the pre-amplifier, SHV is a high-voltage cable connection, and BNC is an adapter for cable connection for voltage pulse signals [11–13]. The two inlet holes (φ12 mm) were made such that the liquid sample, including the radionuclide source, can flow through the front and back sides.

The detector was connected to the dark box in the acrylic scintillator support structure and tube. The top of the detector was covered with black cloth, the lid of the dark box was closed, and additional black cloth was used to cover the dark box to minimize the influence of external light. A plastic scintillator obtained from EPIC CRYSTAL was used, and its thickness was 1 mm [14]. The acrylic scintillator support structure and scintillator were attached using an acrylic adhesive. The experiment was conducted using a sample containing the source after visual confirmation that water was not leaking.

In the case of ^{90}Sr, samples corresponding to activity concentrations of 2.51, 5.02, 7.53, and 10.04 Bq/g were prepared. For ^{3}H, samples corresponding to activity concentrations of 253,206, 506,413, 759,620, and 1,012,827 Bq/g were prepared. The activity concentration of each sample was derived considering the half-life [15].

2.3.1. Experimental setup for flow rate

In the flow-rate experiment, the silicon tube from the front and back sides of the dark box was connected to the peristaltic pump and the flow rate was varied. The flow rate can be measured accurately in the peristaltic pump by calibration. The flow rates were set to 0, 600, 800, and 1000 mL/min. The flow rate was set by

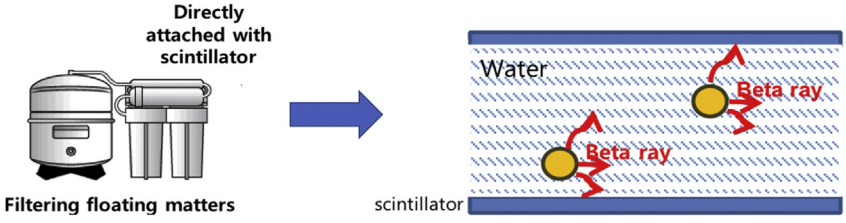

Fig. 1. Schematic of in situ beta monitoring system.

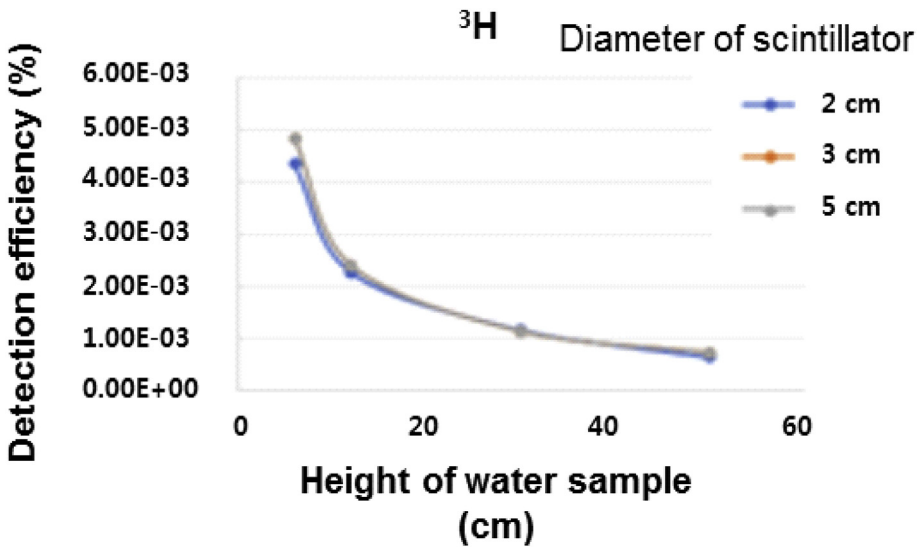

Fig. 2. Detection efficiency according to diameter of scintillator and height of sample.

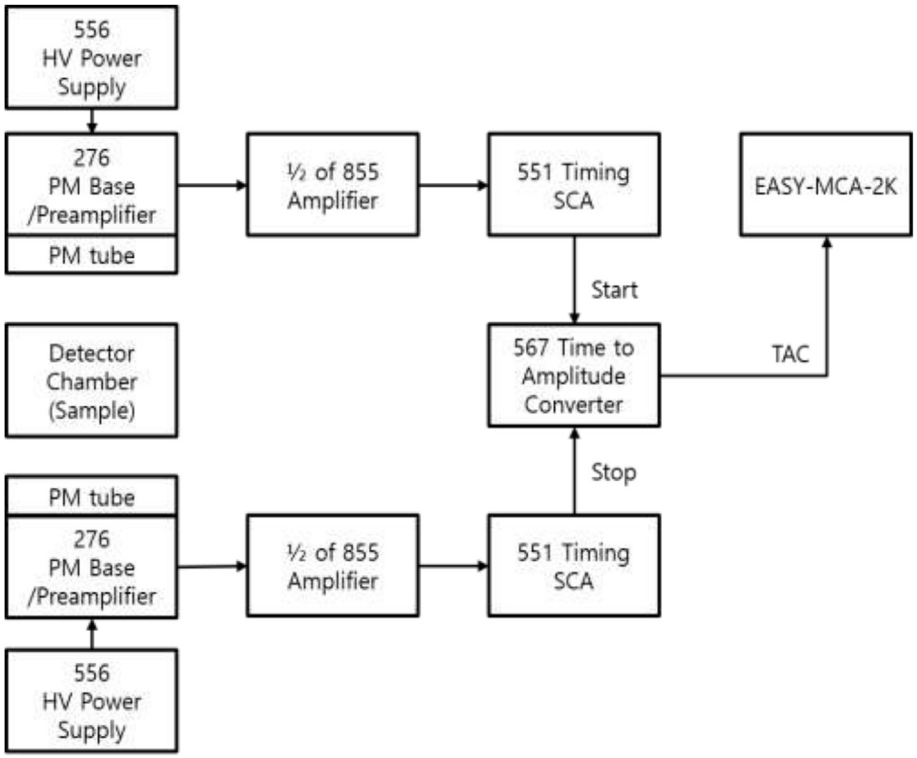

Fig. 3. Configuration of time-delay coincidence circuit for beta detection.

activating the pump to verify the amount of liquid flowing into the acrylic scintillator support structure without any liquid remaining in the pump. For flow rates below 600 mL/min, it was confirmed that the liquid could not pass through the acrylic scintillator support structure. Therefore, the experiments were conducted at flow rates above 600 mL/min.

2.3.2. Experimental setup for amplification

The coarse gain of the 855 dual amplifier was changed to 10, 20, and 40 at a flow rate of 0 mL/min. At a coarse gain of 10, the fine gain was adjusted to 2.5 and 4.0; the fine gain was set to 3.2 and 4.5 for a coarse gain of 20, and 3.9 and 4.9 for a coarse gain of 40.

2.4. Data analysis

Experiments were conducted by deriving the MDA according to change in the flow rate and the degree of amplification of the 855 dual amplifier. The MDA was calculated using equation (1) at 95% confidence interval, and it was confirmed by inputting the background count, measurement time when sample and background measurement time are the same and detection efficiency values obtained from the experiment [3].

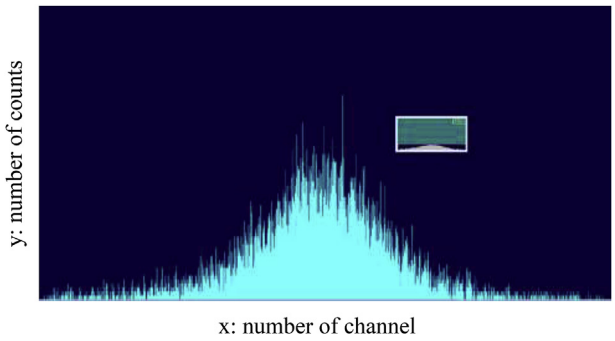

Fig. 4. Example of experiment spectrum.

$$\mathrm{MDA} = \frac{2.71 + 4.65 \times \sqrt{N_b \times T}}{T \times \varepsilon \times 1/100 \times V_c} \quad (1)$$

where

N_b = Background count rate (cps)
ε = Efficiency (%)
T = Sample and background measurement time (s)
V_c = Volume of sample (g/cm^3).

The detection efficiency was derived using equation (2) [2].

$$\varepsilon\,(\%) = \frac{C_g - N_b}{A} \times 100 \quad (2)$$

where

C_g = Gross count rate (cps)
N_b = Background count rate (cps)
A = Activity (Bq).

3. Results and discussions

The flow rate and amplification of the electronic system are the measured parameters and the results are presented in this section.

3.1. Effect of flow rate

First, the change in the background count rate with the flow rate was confirmed using distilled water before the experiment involving injection of the source. As observed in Table 1, there is no significant difference in the background count rate even when the flow rate is varied.

For ^{90}Sr, the highest activity concentration of 10.04 Bq/g was used to derive the MDA reach time as shown in Fig. 5, and an MDA of approximately 1/10 of the actual activity concentration was indicated. When the flow rate was varied in the case where the ^{90}Sr source was actually injected, the activity concentration value to be measured can be confirmed at approximately 40 s for all flow rates. The standard uncertainty of the measured data was 0.60%. Table 1 presents the actual measured background and gross count rates in the experiments involving ^{90}Sr.

For ^{3}H, the highest activity concentration of 1,012,827 Bq/g was used to derive the MDA reach time as shown in Fig. 6, and the MDA was set at approximately 1/10 the value of the actual input activity concentration. The experimental results of the ^{3}H source were similar to those of ^{90}Sr. In the case of the ^{3}H source, the activity

Table 1
Background and gross count rate according to flow rate (Background,^{90}Sr and ^{3}H).

		0 mL/min	600 mL/min	800 mL/min	1000 mL/min
Background count rate (cps)	Background	31.12 ± 0.23	31.12 ± 0.17	31.39 ± 0.12	31.24 ± 0.19
	^{90}Sr	7.60 ± 0.23			
	^{3}H	7.13 ± 0.14			
Gross count rate (cps)	^{90}Sr	33.05 ± 0.12	32.4 ± 0.15	32.88 ± 0.25	32.54 ± 0.19
	^{3}H	15.18 ± 0.20	15.03 ± 0.22	15.72 ± 0.15	15.15 ± 0.20

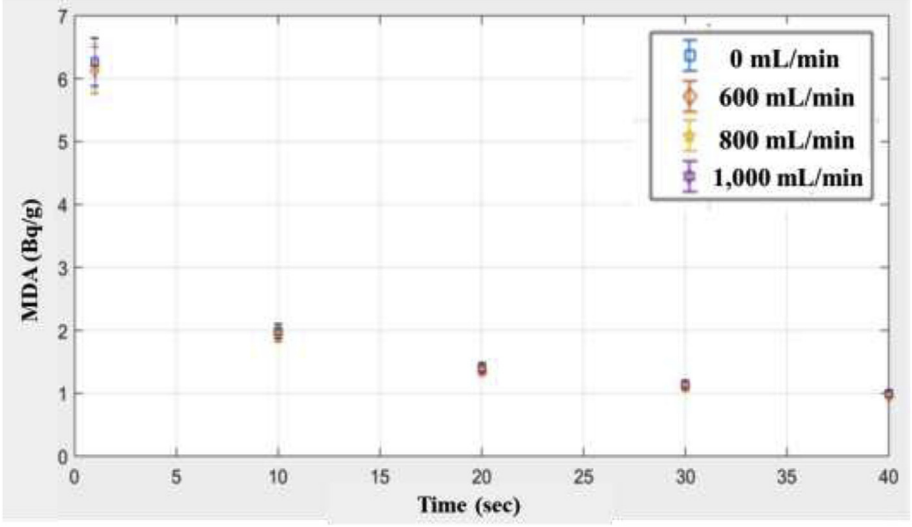

Fig. 5. Analysis of MDA detection by flow rate for ^{90}Sr.

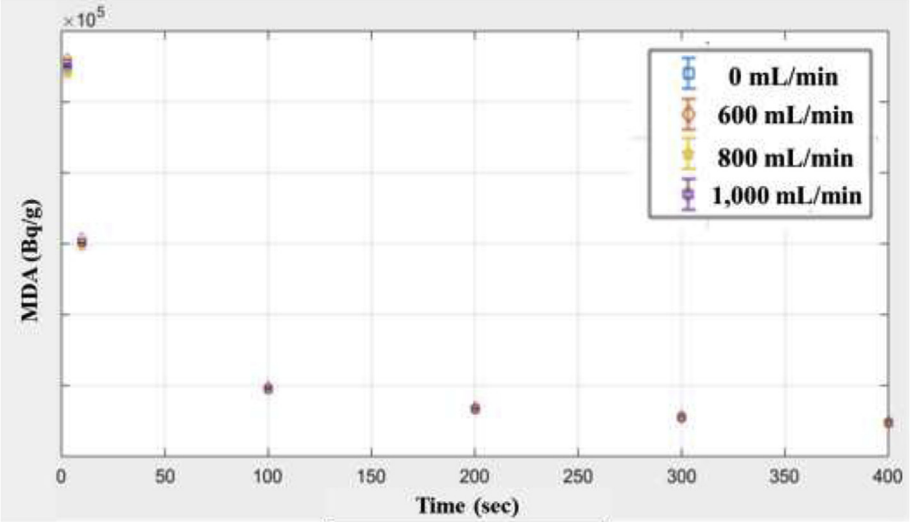

Fig. 6. Analysis of MDA detection by flow rate for ^{3}H.

concentration values to be measured were confirmed at approximately 400 s for all flow rates. The standard uncertainty of the measured data was 0.15%. Table 1 lists the actual measured background and gross count rates in the experiments involving ^{3}H. From the above discussion, it is clear that a change in the flow rate may not be considered in the process of supplying the sample through a pump for actual monitoring.

3.2. Effect of amplification

For ^{90}Sr, the target MDA was set to 1/10 the initial activity concentration (2.51, 5.02, 7.53, and 10.04 Bq/g) as shown in Fig. 7 (a, b, c, and d), and the amplification was varied to derive the required time for measurements. It can be observed that the time required for the MDA to be measured decreases as the degree of amplification increases for all activity concentrations of ^{90}Sr. The coefficients of determination (R^2) of the linearity test for coarse gain values of 10, 20, and 40 were 0.9998, 0.9992, and 0.9954, respectively, and the reliability of the experimental data was confirmed. The measurement uncertainty values for coarse gains of 10, 20, and 40 were 0.60, 0.30, and 0.16%, respectively. Table 2 lists the actual measured background and gross count rates at varying

(a) ^{90}Sr 2.51 Bq/g, MDA for coarse gains of 10, 20, and 40

(b) ^{90}Sr 5.02 Bq/g, MDA for coarse gains of 10, 20, and 40

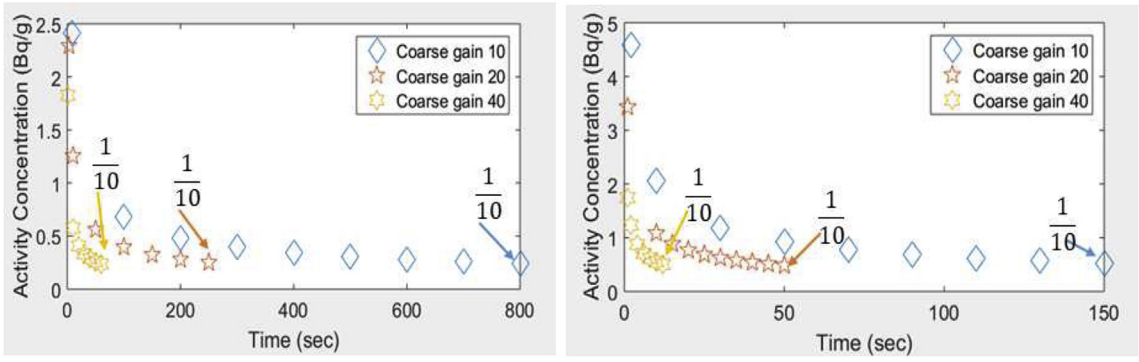

(c) ^{90}Sr 7.53 Bq/g, MDA for coarse gains of 10, 20, and 40

(d) ^{90}Sr 10.04 Bq/g, MDA for coarse gains of 10, 20, and 40

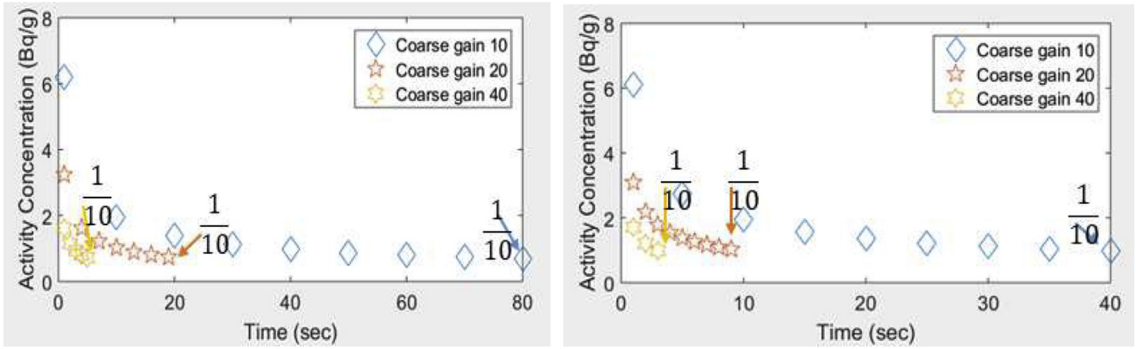

Fig. 7. MDA based on amplification according to ^{90}Sr activity concentration.

Table 2
Count rate of ^{90}Sr according to activity concentration and coarse gain.

^{90}Sr					
Activity Concentration (Bq/g)		2.51	5.02	7.53	10.04
Background count rate (cps)	Coarse gain 10	7.25 ± 0.16	7.41 ± 0.12	7.48 ± 0.11	7.60 ± 0.23
	Coarse gain 20	8.55 ± 0.18	8.04 ± 0.15	8.28 ± 0.11	7.97 ± 0.19
	Coarse gain 40	14.94 ± 0.15	14.97 ± 0.18	15.15 ± 0.17	15.26 ± 0.19
Gross count rate (cps)	Coarse gain 10	12.95 ± 0.18	19.42 ± 0.21	26.32 ± 0.18	33.05 ± 0.12
	Coarse gain 20	18.43 ± 0.14	30.89 ± 0.18	44.63 ± 0.13	58.75 ± 0.10
	Coarse gain 40	36.43 ± 0.17	59.90 ± 0.17	87.78 ± 0.19	106.94 ± 0.19

coarse gains of 10, 20, and 40 for activity concentrations of 2.51, 5.02, 7.53, and 10.04 Bq/g.

For ^{3}H, the target MDA was set to 1/10 the initial activity concentration (253,206, 506,413, 759,620, and 1,012,827 Bq/g) as shown in Fig. 8 (a, b, c, and d), and the amplification was varied to derive the required time for measurement. As in the case of ^{90}Sr, the time required for the MDA to be measured decreases for ^{3}H as the degree of amplification increases at all activity concentrations. The R^2 values of the linearity test for coarse gains of 10, 20, and 40 were 0.9992, 0.9711, and 0.9934, respectively, and the reliability of the experimental data was confirmed. The measurement uncertainty values for coarse gains of 10, 20, and 40 were 0.15, 0.13, and 0.55%, respectively. Table 3 presents the actual measured background and gross count rates at varying coarse gains of 10, 20, and 40 for activity concentrations of 253,206, 506,413, 759,620, and 1,012,827 Bq/g.

It can be observed from the above results that the background and gross count rates of ^{90}Sr and ^{3}H are changed by the degree of amplification. The results indicate increase in the background and gross count rates; however, the increase in the gross count rate is significantly larger than that of background count rate.

The clearance level for ^{90}Sr is 1 Bq/g (1000 Bq/L) and that of ^{3}H is 100 Bq/g (100,000 Bq/L) [16]. The time required to measure 0.1 Bq/g (100 Bq/L) and 10 Bq/g (10,000 Bq/L), which correspond to 1/10 of the clearance levels of ^{90}Sr and ^{3}H, are 5 min and approximately 2 y for ^{90}Sr and ^{3}H, respectively. The background count, detection efficiency, and internal volume of the acrylic scintillator support structure, which are factors affecting the MDA, must be controlled to improve the field application of tritium detection in groundwater. The measurement time can be reduced by changing the internal volume of the scintillator support structure designed and manufactured for the in-situ measurement system. That is, the structure of the detector can be easily changed, and the time required to reach the MDA to be measured can be reduced by changing the shape of the plastic scintillator and the type of PMTs. Different from the LSC method, which includes a pretreatment process, this approach offers the advantage of real-time on-site monitoring.

In the case of ^{90}Sr, it is possible to perform real-time monitoring in the field, whereas real-time monitoring is not possible in the case

(a) ^{3}H 253,206 Bq/g, MDA for coarse gains of 10, 20, and 40

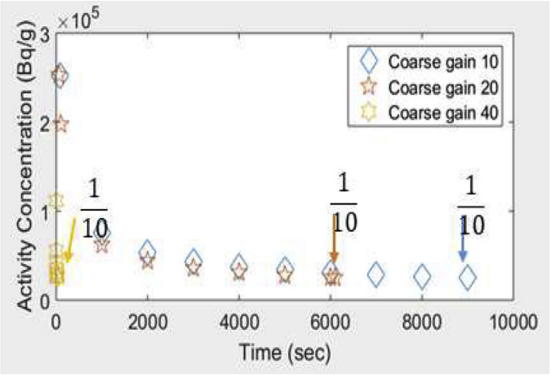

(b) ^{3}H 506,413 Bq/g, MDA for coarse gains of 10, 20, and 40

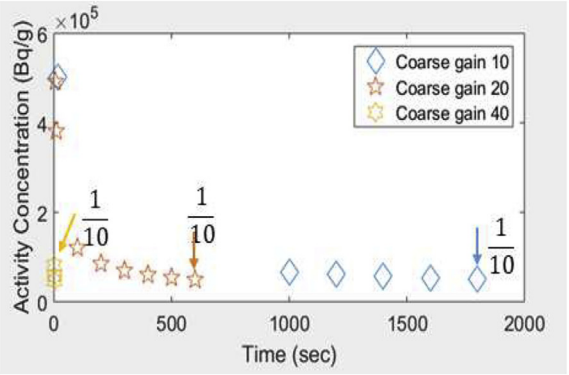

(c) ^{3}H 759,620 Bq/g, MDA for coarse gains of 10, 20, and 40

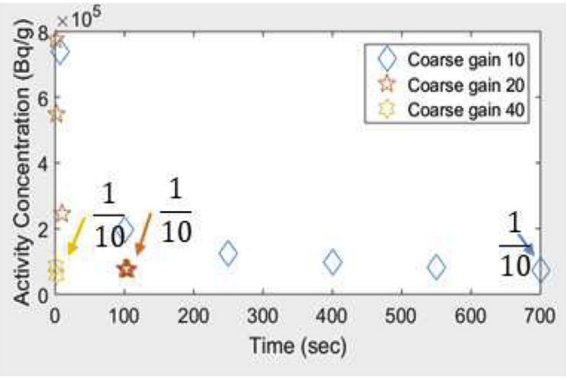

(d) ^{3}H 1,012,827 Bq/g, MDA for coarse gains of 10, 20, and 40

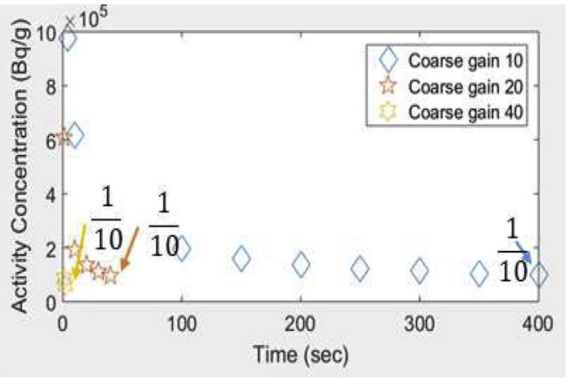

Fig. 8. MDA based on amplification according to ^{3}H activity concentration.

Table 3
Count rate of ^{3}H according to activity concentration and coarse gain.

^{3}H					
Activity Concentration (Bq/g)		253,206	506,413	759,620	1,012,827
Background count rate (cps)	Coarse gain 10	7.19 ± 0.12	7.40 ± 0.15	7.19 ± 0.14	7.13 ± 0.14
	Coarse gain 20	9.59 ± 0.19	9.80 ± 0.18	10.07 ± 0.15	10.09 ± 0.21
	Coarse gain 40	15.36 ± 0.17	15.26 ± 0.14	14.99 ± 0.22	14.33 ± 0.18
Gross count rate (cps)	Coarse gain 10	8.83 ± 0.10	11.09 ± 0.12	13.22 ± 0.14	15.18 ± 0.18
	Coarse gain 20	11.58 ± 0.11	16.32 ± 0.16	25.28 ± 0.18	35.95 ± 0.23
	Coarse gain 40	50.6 ± 0.18	111.50 ± 0.26	154.01 ± 0.28	199.12 ± 0.19

of ^{3}H because the time to reach the MDA is too long. Therefore, in the future, ^{3}H should be measured in a gaseous state using polymer electrolyte membrane (PEM) electrolysis method [17]. At 0 °C and 1 atm, the densities of hydrogen gas and water are 0.0899 g/L and 999 g/L, respectively, which reduces the effect of self-absorption to about 1/10,000. The sensitivity can be improved by a factor of 10 compared to the conventional method by increasing the volume through electrolysis owing to reduction in the self-absorption effect, even if the concentration is reduced to about 1/1000. Improving the sensitivity by a factor of 10 has the effect of decreasing the measurement time to 1/90 to obtain the same level of sensitivity. In addition, the influence of disturbance by water contaminated radionuclides can be minimized as only pure hydrogen is extracted solely through electrolysis.

4. Conclusion

In this study, a monitoring system for in situ beta measurements in water was designed and constructed. The process of quantizing the MDA was carried out corresponding to a particular flow rate and amplification. The flow rate had no effect on the MDA; hence, it is expected that the time to reach the MDA can be reduced by optimizing the amplification and this concept can be applied in rapid monitoring systems.

On the basis of the MDA equation, the background count was intended to reduce approximately 1/5 using shielding material, increase the active area of the detection part, and increase the detection efficiency by approximately a factor of two using PMT with good detection efficiency.

In the case of ^{90}Sr, the time to reach the MDA to be measured is suitable for real-time monitoring, but additional experiments are needed to achieve real-time monitoring for ^{3}H. If the detection part is redesigned according to the MDA equation and the PEM electrolysis method is used, then, real-time monitoring for ^{3}H is possible.

Acknowledgments

This work was supported by the National Research Foundation of Korea (NRF) grant funded by the Korean government (MSIP: Ministry of Science, ICT and Future Planning) NRF-2016M2B2B1945082, NRF-22A20153413555.

Appendix A. Supplementary data

Supplementary data to this article can be found online at https://doi.org/10.1016/j.net.2019.02.001.

References

[1] S.W. Duce, H. Amir, M.L. Mohagheighi, L.M. Mark, R.R. Robert, R.M. David, In situ radiation detection demonstration, in: WM'00 Conference, Tucson, AZ, February 27 −, March 2, 2000.
[2] S.J. Ko, et al., Radiation Detection & Measurement, 2001 (in Korean language).
[3] S. Croft, et al., The estimation of the minimum detectable activity from measured passive neutron coincidence counter data, in: Proc. 46th Int. Symp. on Nuclear Material Management (INMM), 2005.
[4] T.T. Alton, S.D. Monk, D. Cheneler, Beta particle energy spectra shift due to self-attenuation effects in environmental sources, Nucl. Eng. Technol. 49 (2017) 1483–1488.
[5] Ortec Inc. AN34 Experiment 9 Time Coincidence Techniques and Absolute Activity Measurements. https://www3.nd.edu/~wzech/Application-Note-AN34-Experiments-Nuclear-Science-Experiment-9.pdf.
[6] Ortec Inc. Model 556H High Voltage Power Supply Operating and Service Manual. https://www.ortec-online.com/-/media/ametekortec/manuals/556h-mnl.pdf.
[7] HAMAMATSU, Photomultiplier tube R878. www.hamamatsu.com.
[8] Ortec Inc. Model 855 Dual Spectroscopy Amplifier Operating and Service Manual. https://www.ortec-online.com/-/media/ametekortec/manuals/855-mnl.pdf.
[9] Ortec Inc. Model 551 Timing Single-Channel Analyzer Operating and Service Manual. https://www.ortec-online.com/-/media/ametekortec/manuals/551-mnl.pdf.
[10] Ortec Inc, EASY-MCA-8KTM EASY-MCA-2KTM digital gamma-ray spectrometer user's manual. https://www.ortec-online.com/-/media/ametekortec/manuals/easy-mca-mnl.pdf.
[11] PASTERNACK, RF Adapters Technical Data Sheet (PE9336).
[12] PASTERNACK, RF Adapters Technical Data Sheet (PE9363).
[13] http://rarecomponents.com/store/1017,Search:19-March-2018.
[14] Saint-Gobain Crystals, Organic Scintillation Materials. https://www.crystals.saint-gobain.com/products/organic-scintillation-materials, 2014.
[15] P. Alaei, Introduction to health physics, Med. Phys. 35 (2008), 5959-5959.
[16] http://www.nssc.go.kr/nssc/information/law4_4.jsp, The code of nuclear safety and security commission JAE2012-59Ho: Regulation for the clearance of radioactive waste (2015).
[17] A. Soreefan, Development of an Original Laboratory Prototype for a Field Tritium Detector Containing a PEM Electrolyzer Mounted in Series with a Gas Proportional Counter, 2009.